Goal-directed action preparation in humans entails a mixture of corticospinal neural computations

Corey G. Wadsley[1,2], Thuan Nguyen[3], Chris Horton[1], Ian Greenhouse[1,2,*]

[1]Action Control Lab, Department of Human Physiology, University of Oregon, Eugene, Oregon, USA
[2]Institute of Neuroscience, University of Oregon, Eugene, Oregon, USA
[3]School of Public Health, Portland State University-Oregon Health and Science University, Portland, Oregon, USA

**Corresponding author*: Ian Greenhouse (img@uoregon.edu)
Department of Human Physiology
181 Esslinger Hall,
1525 University St.
Eugene, OR 97403

Keywords: Human, Motor cortex, Action preparation, Gain modulation, Noninvasive brain stimulation

Running title: Human action preparation entails corticospinal neural computations

Key points:

- Neural computations determine what information is transmitted through brain circuits.
- We investigated whether the motor system uses computations similar to those observed in sensory systems by noninvasively stimulating the corticospinal pathway in humans during goal-directed action preparation.
- We discovered physiological evidence that corticospinal projections to behaviorally relevant muscles exhibit nonlinear gain computations, while projections to behaviorally irrelevant muscles exhibit linear suppression.
- Our findings suggest that certain computational principles generalize to the human motor system and serve to enhance the contrast between relevant and background neural activity.
- These results indicate that neural computations during goal-directed action preparation may support motor control by increasing signal-to-noise within the corticospinal pathway.

Abstract:

The seemingly effortless ability of humans to transition from thinking about actions to initiating them relies on sculpting corticospinal output from primary motor cortex. This study tested whether canonical additive and multiplicative neural computations, well-described in sensory systems, generalize to the corticospinal pathway during human action preparation. We used non-invasive brain stimulation to measure corticospinal input-output across varying action preparation contexts during instructed-delay finger response tasks. Goal-directed action preparation was marked by increased multiplicative gain of corticospinal projections to task-relevant muscles and additive suppression of corticospinal projections to non-selected and task-irrelevant muscles. Individuals who modulated corticospinal gain to a greater extent were faster to initiate prepared responses. Our findings provide physiological evidence of combined additive suppression and gain modulation in the human motor system. We propose these computations support action preparation by enhancing the contrast between selected motor representations and surrounding background activity to facilitate response selection and execution.

Abstract figure

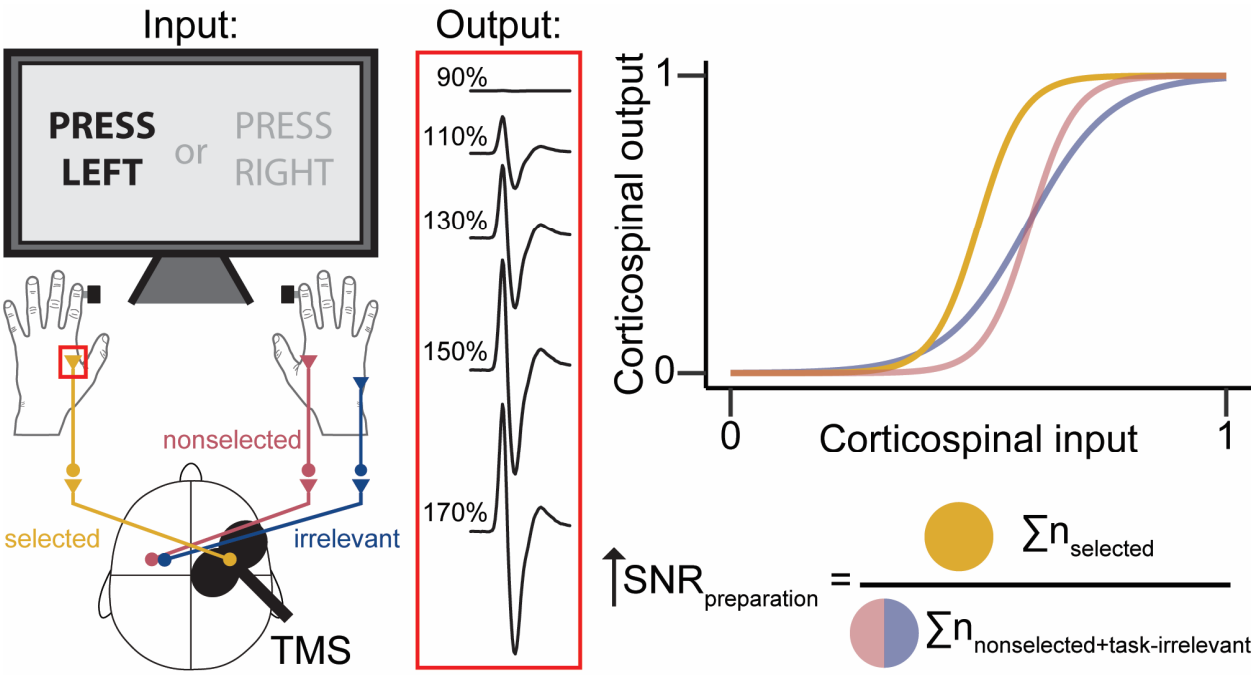

Abstract figure legend. Goal-directed action preparation shapes corticospinal output across selected, nonselected, and task-irrelevant motor representations. This study examined whether additive and multiplicative neural computations, common in sensory systems, occur within the corticospinal pathway during action preparation. We probed corticospinal input-output during the performance of various instructed-delay response tasks by applying a range of transcranial magnetic stimulation (TMS) intensities (input) over the primary motor cortex and measuring the resultant motor-evoked potentials (output) from the hand. We found that goal-directed action preparation increases corticospinal gain multiplicatively in task-relevant motor representations while additively suppressing nonselected and irrelevant representations. Greater gain modulation predicted faster responses, highlighting how these computations can enhance signal-to-noise (SNR) to enable efficient action selection and execution in the human motor system.

Introduction

Humans are experts at using their fingers for goal-directed actions to interact with their environment effectively (Xu *et al.*, 2024). This behavioral repertoire is supported by a specially evolved neural architecture comprising excitatory and inhibitory mechanisms that sculpt corticospinal (CS) pathway output during goal-directed action preparation (Prut & Fetz, 1999; Duque *et al.*, 2017; Bundt & Huster, 2024). The anatomy of the distributed cortical and spinal circuits that modulate CS output during action preparation and execution is well characterized (Wang *et al.*, 2017; Derosiere & Duque, 2020). However, the precise neural computations that unfold throughout the transition from action preparation to execution are not (Churchland & Shenoy, 2024). Candidate computations have been proposed but are based on neuronal circuit modeling and experimental evidence from investigations of non-motor neural systems and behaviors (Greenhouse, 2022). Thus, it is unclear whether computational principles from non-motor circuits generalize to the human motor system and account for the top-down modulation of CS output during action preparation.

Influential models of goal-directed action preparation postulate that inhibition of the CS pathway acts as a functional gate, with the removal of inhibition allowing selective excitatory signals to pass through to the musculature and produce intended actions (Zagha *et al.*, 2015; Soteropoulos, 2018). Yet, physiological recordings from non-human primates have provided mixed evidence for gating mechanisms within the CS pathway (Merchant *et al.*, 2008; Kaufman *et al.*, 2010, 2013). Indeed, (dis)inhibition supports a variety of computations other than gating in non-motor neural circuits (Katzner *et al.*, 2011; Lee *et al.*, 2012; Mischler *et al.*, 2023). Multifaceted computations are also likely required in the motor system since movements are not static but instead defined by various kinetic and kinematic features that characterize a given action. Therefore, alternative interpretations to the functional gating account should be considered to better explain how preparatory activity determines CS pathway excitability to shape ensuing actions.

The selection and timing of goal-directed actions may be determined by neural computations similar to, or bound to, those of non-motor circuits (Beste *et al.*, 2023). Such computations, responsible for sculpting descending signals, are expected to manifest in distinct patterns of CS input-output during

goal-directed action preparation. One candidate computation is gain modulation, defined in studies of sensory processing as a multiplicative (non-linear) change in a system‘s input-output relationship and a proposed feature of canonical normalization processes within the brain (Hillyard *et al.*, 1998; Salinas & Thier, 2000; Pi *et al.*, 2013). Computational models indicate gain modulation is important in determining primary motor cortex (M1) output (Pouget & Snyder, 2000; Stroud *et al.*, 2018), the predominant source of descending signals of the human CS tract (Welniarz *et al.*, 2017). Additive modulation, defined by a linear shift across an input-output spectrum (Silver, 2010), is an alternative candidate computation that may account for CS input-output adjustments during action preparation. Computational models of additive modulation indicate effective changes in an input-output threshold (Mitchell & Silver, 2003), whereby widespread suppression can stabilize a neuronal population by reducing the preponderance of spontaneous firing (Ferguson & Cardin, 2020). During action preparation, additive modulation may function as the ‘quiet before the storm’ to prepare the CS pathway for impending descending commands.

A third alternative is that multiplicative and additive computations are concurrent and complementary. A precedent for synergistic computations can be found in the vision system. Extending a divisive normalization framework (Carandini & Heeger, 2012) to the motor system, the activity of a motor representation selected for action can be divided by the summed activity of alternative non-selected and bystander motor representations, producing enhanced signal-to-noise (Georgopoulos & Stefanis, 2007; Greenhouse, 2022). A combination of multiplicative and additive computations could serve to separate figure from ground in a manner resembling neural sensory processing and would be consistent with a general neurocomputational principle throughout the human nervous system akin to exponentiation, linear filtering, and divisive normalization (Carandini & Heeger, 2012).

Evidence from transcranial magnetic stimulation (TMS) studies indicates that the motor system engages modulatory processes analogous to those of sensory systems. TMS is a noninvasive brain stimulation technique used to elicit motor-evoked potentials (MEPs) as an index of CS output (Bestmann & Duque, 2016). Seminal studies have demonstrated surround inhibition of MEPs within the CS pathway, whereby selected motor representations are potentiated while surround representations are suppressed during action initiation (Stinear & Byblow, 2003; Sohn & Hallett, 2004). Such surround inhibition is thought

to ‘sharpen’ motor representations (Georgopoulos & Stefanis, 2007), a motif that resembles surround suppression observed consistently in the visual (Allman *et al.*, 1985; Angelucci *et al.*, 2017), auditory (Wang *et al.*, 2012; Gilday *et al.*, 2023), somatosensory (Foeller *et al.*, 2005), and olfactory (Aungst *et al.*, 2003) systems. Other TMS studies have identified distinct modulation of MEPs via intra-hemispheric and inter-hemispheric mechanisms across various action preparation contexts (e.g., Derosiere & Duque, 2020). However, these studies have typically used a fixed intensity and could not determine whether MEP modulation is part of additive or multiplicative computations across the entire CS input-output spectrum. Therefore, it remains unclear whether the human CS pathway performs canonical additive and multiplicative computations during action preparation.

In this study, we tested the presence of multiplicative and additive computations in human CS input-output during the behavioral state change from rest to action preparation of goal-directed finger movements (Figure 1a). We hypothesized that goal-directed action preparation involves a concurrent gain increase and additive suppression to enhance the contrast between selected and background motor representations along the CS pathway. To test this hypothesis, we used TMS to noninvasively probe the CS input-output of a target hand motor representation during instructed-delay reaction time tasks. These tasks involved either a choice between two fingers within one hand or between the two hands making it possible to evaluate CS input-output across various contexts, including when the same stimulated motor representation was selected, nonselected but task-relevant, or entirely task-irrelevant to action preparation. This design enabled us to characterize computations within the same CS pathway under different behavioral contexts.

Methods

Ethical Approval

The study was approved by the University of Oregon Institutional Review Board (Study ID 10182017.017) and conformed to the standards set by the *Declaration of Helsinki*, except for registration in a database. All procedures were performed with each participant's understanding and written consent.

Participants

Forty-five young, neurologically healthy adults volunteered to participate. All participants self-reported as right-handed and were screened for contraindications to TMS before data collection. Five participants were excluded from data collection due to a high resting motor threshold (≥ 60% maximum stimulator output), making the TMS input-output protocol unfeasible. An additional participant was excluded after data collection due to noncompliance with task instructions. The remaining 39 participants completed the entire study and were available for all statistical analyses (20 females, 19 males; mean age 20.3 yrs., range 18 to 30 yrs.).

Task protocol

Goal-directed action preparation was assessed with an instructed-delay two-choice reaction time task (Figure 1b). Participants were seated comfortably in front of a computer monitor (59 Hz refresh rate, ~60 cm viewing distance) with their hands palm-down and shoulder-width apart on a table surface. The task was designed using Psychtoolbox-3 integrated with MATLAB (R2019b; The MathWorks) and a custom response board (Makey Makey v.1.2; Joylabz) for accurate timing. Stimuli were synchronized with task equipment through an analog-to-digital data-acquisition module (PCI-6620; National Instruments) and verified during later offline analyses using photodiode recordings. The default task display consisted of a blank grey background at trial onset. A fixation cue (centered white rectangle, 20 x 20 pixels) appeared 0.3 s after trial onset. A warning cue appeared 1 to 1.5 s after trial onset (randomly drawn from a uniform distribution) and indicated the forthcoming response (hollow leftward or rightward pointed triangle, 140 x 150 pixels). An imperative stimulus (triangle filling white) appeared 0.9 s after the warning cue and lasted until a button press was recorded or 0.8 s elapsed. Each trial was followed by an intertrial interval (blank grey background) after the imperative stimulus and lasted until 7.6 s had elapsed from the trial onset.

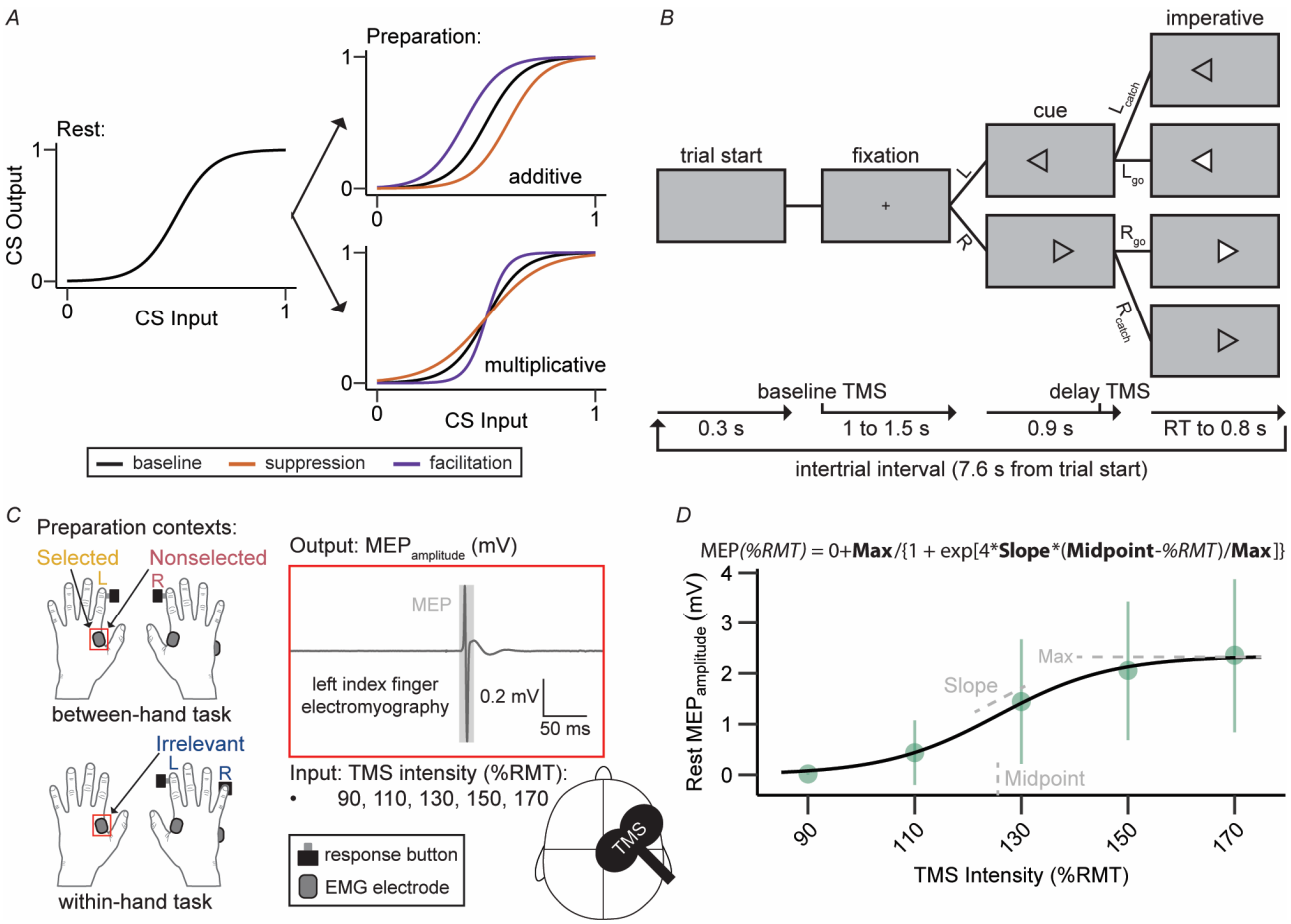

Figure 1: Assessment of human CS input-output during goal-directed action preparation. **a**, Corticospinal (CS) input-output can exhibit additive and/or multiplicative modulation from baseline rest to a preparatory state. **b**, Goal-directed action preparation was assessed with an instructed-delay two-choice reaction time task requiring left (L) or right (R) responses. Most trials were go trials during which the imperative stimulus appeared until a reaction time (RT) was recorded or 0.8 s elapsed. A subset of catch trials (~8%) was included to prevent participants from predicting imperative stimulus onset. **c**, The experiment was split into between-hand and within-hand tasks, enabling the assessment of CS output from the left index finger with single-pulse transcranial magnetic stimulation (TMS) when the targeted motor representation was at baseline and when it was selected, nonselected, or irrelevant for action preparation. Here, input was TMS intensity relative to a participant's resting motor threshold (%RMT), and output was the amplitude of ensuing motor evoked potentials (MEPs). **d**, CS input-output curves derived from pre-task resting state MEP data (n = 39) and fit with a population-based nonlinear mixed effects model using a three-parameter Boltzmann function. Green dots and error bars indicate mean MEP amplitude ± standard deviation at each TMS intensity. Dashed grey lines illustrate parameter estimates.

The experiment was split into between-hand and within-hand choice tasks (Figure 1c). Both tasks were performed in the same session with a counterbalanced order across participants. Participants were provided a short break in between tasks. Left and right imperative stimuli required button presses from the left and right index fingers during the between-hand choice task and button presses from the right index and pinky fingers during the within-hand task. Participants were instructed to relax during the fixation period, to prepare but not execute the forthcoming response during the cue period, and to execute the cued response as fast as possible when the imperative stimulus was presented. A subset of no-go catch trials (i.e., no imperative stimulus; 8% of trials) was included to discourage participants from

123 responding prematurely in anticipation of the imperative stimulus. For each task, there was a total of 238
124 trials evenly distributed across left and right imperative stimuli and split across 4 blocks alternating
125 between 59 and 60 trials. The entire experiment lasted 2.5 hours on average.

126 *Electromyography*

127 Electrophysiological muscle activity was assessed with surface electromyography (EMG)
128 recorded using bipolar Ag-AgCl surface electrodes (Delsys Incorporated). EMG was collected in a copper
129 Faraday cage to minimize electrical noise in EMG recordings. Electrodes were placed on the left and right
130 FDI and the right *abductor digiti minimi* (ADM) hand muscles, which corresponded to the primary agonist
131 muscles for between-hand$_{left}$ (left FDI), between-hand$_{right}$ and within-hand$_{left}$ (right FDI), and within-hand$_{right}$
132 (right ADM) choice alternatives. An additional EMG electrode was positioned over the C3 vertebra of the
133 neck to record TMS artifacts, and a shared ground electrode was positioned on the left ulnar styloid
134 process. EMG activity was amplified (×1000), bandpass filtered (20 – 450 Hz), baseline-corrected to 0
135 mV, and sampled at 5000 Hz with a Bagnoli-8 amplifier (Delsys Incorporated) connected to a BNC-2090A
136 terminal block (National Instruments). EMG data were recorded and monitored on each trial for 4 s from
137 onset using the MATLAB-based VETA toolbox (Jackson & Greenhouse, 2019) and stored for later offline
138 analyses.

139 *Transcranial Magnetic Stimulation*

140 Physiological changes in CS input-output during goal-directed action preparation were assessed
141 with single-pulse TMS delivered using a 70 mm figure-of-eight coil connected to a MagStim 200^2
142 stimulator (MagStim Ltd.). The coil was oriented to induce a posterior-to-anterior flowing current in the
143 underlying cortical tissue. The optimal coil position ('motor hotspot') over right M1 for eliciting a motor
144 evoked potential (MEP) in the left FDI was then assessed and marked on the scalp. The resting motor
145 threshold (RMT) of left FDI was defined as the minimum stimulator output required to elicit an MEP
146 amplitude of at least 0.05 mV at rest using a maximum-likelihood parameter estimation by sequential
147 testing strategy (Silbert *et al.*, 2013). TMS was delivered across a range of stimulation intensities (90%,
148 110%, 130%, 150%, and 170%; 14 stimuli per intensity) relative to a participant's RMT (mean 43.4 ± 7.0

149 % maximum stimulator output) to derive CS input-output curves, with MEP peak-to-peak amplitude used
150 as an index of CS output (Bestmann & Duque, 2016). The TMS input-output protocol was performed at
151 baseline and delay time points in both the between-hand and within-hand tasks. Baseline TMS coincided
152 with the onset of the fixation cue (i.e., end of intertrial interval) to evaluate resting CS output within a task
153 context but before any trial-relevant information was provided (Bakken *et al.*, 2024). Delay TMS was
154 delivered 100 ms before the imperative stimulus (i.e., 800 ms into the cue period) to evaluate CS output
155 during action preparation and, in related tasks, corresponds to a time point of maximal MEP modulation
156 before transition to action execution (Lebon *et al.*, 2016). The above task design enabled assessment of
157 CS output to the left FDI muscle during baseline and during action preparation when the muscle was
158 selected (i.e., the agonist for prepared action), nonselected, or task-irrelevant (Figure 1c). Nonselected
159 refers to the context in which the left index finger was a choice alternative in the task but was not cued to
160 respond on a given trial, while task-irrelevant refers to the context in which the left index finger was never
161 a choice alternative in the task. Here, we conceptualize the left FDI as task-relevant in both selected and
162 nonselected contexts since CS output is modulated differently when an effector is part of a task set than
163 when it is task-irrelevant entirely (Greenhouse *et al.*, 2015).

164 *Dependent measures*

165 Data were preprocessed using the VETA toolbox in two stages. In the first stage, EMG bursts,
166 MEPs, and TMS artifacts were marked with the automated detection *findEMG.m* function. In the second
167 stage, data was manually reviewed using the *visualizeEMG.m* function to ensure the accuracy of EMG
168 measures. Here, EMG data contaminated by artifacts (e.g., electrical noise, pre-TMS muscle activity)
169 were rejected, and EMG burst onset timings were adjusted when required. Dependent measures were
170 then extracted with custom scripts in MATLAB. Behavioral measures were analyzed from nonstimulated
171 and stimulated trials separately to account for the potential influence of TMS on motor output (Foltys *et*
172 *al.*, 2001). Go success was calculated as the percentage of go trials where a correct response was made
173 within 0.8 s from imperative stimulus onset. Catch trial success was calculated as the percentage of no-
174 go trials where the cued response was withheld correctly. Trials with button press RTs less than 100 ms
175 or EMG RTs less than 50 ms were then marked as premature responses and excluded from subsequent

analyses (*M* = 5.8 % of nonstimulated and 13.7% of stimulated trials, respectively). There was a positive correlation between button press and EMG RT for nonstimulated ($r = 0.68$, $P < 0.001$) and stimulated trials ($r = 0.54$, $P < 0.001$), as such, we report only EMG-based RTs for subsequent analyses since it is free from electromechanical delays.

Dependent measures from stimulated trials during the between-hand and within-hand choice tasks included pre-trigger root mean square EMG and MEP amplitudes. In addition to manually reviewing with the VETA toolbox, remaining TMS trials were excluded when average pre-trigger root mean square EMG activity exceeded 30 μV in a -30 to -5 ms pre-TMS window or when outlier MEP amplitudes were identified, defined as values more than three times the scaled median absolute deviation from the median. A mean of 11.4 % of stimulated trials were removed during preprocessing. The mean pre-TMS root mean square EMG activity of the left FDI was then calculated from the remaining trials for each preparation context, collapsed across stimulation intensities. CS output of the left FDI was calculated as the mean MEP peak-to-peak amplitude for each preparation context and stimulation intensity separately.

Statistical analyses

Statistical analyses were performed using R software (Version 4.3.0). The normality of data and model-averaged residual plots were visually inspected where appropriate. Logarithmic transformations were applied to non-normally distributed data, after which model-averaged residual plots were re-evaluated for normality before hypothesis testing. The alpha level was set to 0.05 for statistical significance. P-values for pairwise post-hoc comparisons were obtained using estimated marginal means for mixed-effects models and adjusted for multiple comparisons using the Benjamini-Hochberg method to control the false discovery rate at 5%. In-text data are presented as nontransformed mean ± standard deviation unless otherwise specified.

We employ a population-based nonlinear mixed-effects model to determine the influence of action preparation context on the CS input-output relationship. A modified three-parameter Boltzmann sigmoid function (Heusser *et al.*, 2021) was used to model the nonlinear sigmoidal input-output relationship between TMS intensity and MEP amplitude (Kukke *et al.*, 2014):

$$MEP(\%RMT) = 0 + Max/\{1 + exp[4 * Slope * (Midpoint - \%RMT)/Max]\}$$

where MEP(%RMT) is the predicted MEP peak-to-peak amplitude at a given TMS intensity, calculated as a function of Max (upper plateau), Midpoint (inflection point), and Slope (maximum rate of change) input-output parameter estimates. Here, the Midpoint and Slope parameters indicate additive and multiplicative computations, respectively (Figure 1d). The lower plateau of CS input-output was constrained to 0 mV for greater biological plausibility (i.e., MEP amplitude cannot be negative and should always be 0 mV at a 0% TMS intensity) and provided a better fit of the data compared to an unconstrained model (constrained AIC: 1307.5, unconstrained AIC: 1317.0).

Initial parameter estimates for the nonlinear mixed-effects models were derived from pre-task resting state data to ensure independence between model optimization and statistical analyses. Specifically, initial estimates were set to mean MEP amplitude at 170% RMT for Max, median stimulation intensity for Midpoint (i.e., 130% RMT), and the linear gradient between 110% and 130% RMT for Slope based on visual inspection of averaged MEP amplitude data. We then applied nonlinear least squares modeling (*nls* function in R) with these initial parameter estimates to obtain corresponding optimal parameter estimates of 2.34 mV for Max, 125.6 %RMT for Midpoint, and 0.055 mV/%RMT for Slope with an iterative numerical integration procedure. These estimates were subsequently applied to a model of in-task TMS data (*nlme* function in R). Max, Midpoint, and Slope parameters were estimated from this random intercept model to account for participant variability. The model was then updated with the fixed effect of Context (baseline, irrelevant, nonselected, selected) to examine the influence of action preparation context on CS input-output. Updated models with the fixed effect of Task Order (within-hand first, between-hand first) or Sex (male, female) were also included to determine any effects of task order or participant sex on CS input-output parameters.

A linear mixed-effects model with a fixed effect of Context (baseline, irrelevant, nonselected, selected) was used to confirm that modulation of CS input-output was not attributable to shifts in pre-TMS root mean square EMG activity. An additional analysis of raw MEPs was included to determine the prevalence of preparatory suppression, defined by a reduction in MEP amplitude relative to baseline

228 (Duque & Ivry, 2009), across the CS input-output spectrum. Here, we used paired Wilcoxon-signed rank
229 tests to compare the mean MEP amplitude for a given preparation context to the baseline context for
230 each suprathreshold stimulation separately.

231 Go and catch trial success rates for nonstimulated and stimulated trials were analyzed separately
232 using an omnibus Friedman test with the factor of Response (within-hand$_{left}$, within-hand$_{right}$, between-
233 hand$_{left}$, between-hand$_{right}$) to verify task performance was high and consistent across response
234 alternatives. Nonstimulated and stimulated trial EMG RT was analyzed using a linear mixed-effects model
235 with fixed effects of Task (within-hand, between-hand) and Side (left, right) and random effect of
236 participant specificity to verify participants were responding fast and to determine any differences
237 between tasks and response alternatives.

238 We then estimated a Gain Index *post priori* for each participant to capture interindividual
239 differences in CS input-output Slopes and evaluate whether observed context-dependent gain
240 adjustments correlated with task behavior. Direct parameter estimations could not be used from the
241 population-based model since variance is shared across participants and, thus, interindividual differences
242 between contexts derived from the population-based model are not meaningful. As such, we estimated
243 the Gain Index by 1) extracting the estimated Midpoint for each context and participant separately, 2)
244 determining the two neighboring input TMS intensities (e.g., 110% and 130% RMT if the estimated
245 Midpoint was within these bounds), 3) estimating the linear gradient (slope) between the mean MEP
246 amplitudes from their individual data corresponding to the selected input TMS intensities, and 4)
247 calculating the estimated difference between task-relevant contexts (average of selected and nonselected
248 contexts) and task-irrelevant contexts, normalized to baseline, i.e. ($slope_{relevant}$ - $slope_{irrelevant}$)/$slope_{baseline}$.
249 Thus, a greater Gain Index reflects a larger difference in the Slope of CS input-output between task-
250 relevant and task-irrelevant preparation contexts. The association between mean EMG RT across
251 response options and the Gain Index was then tested using Pearson's correlation for nonstimulated and
252 stimulated trials separately. The average number of trials available for EMG RT analyses were
253 comparable across response options for both nonstimulated (between-hand$_{left}$ 10.6 ± 1.8; between-

254 $hand_{right}$ 11.7 ± 0.7; within-$hand_{left}$ 11.8 ± 0.5; within-$hand_{right}$ 11.8 ± 1.0) and stimulated (between-$hand_{left}$
255 91.6 ± 13.2; between-$hand_{right}$ 92.3 ± 7.0; within-$hand_{left}$ 93.7 ± 7.4; within-$hand_{right}$ 93.8 ± 6.8) trials.

256 **Results**

257 CS input-output parameters changed during goal-directed action preparation in a context-
258 dependent manner (Figure 2a). The Context model provided a better fit of the data than the Null model
259 (Context AIC: 1264.3, Null AIC: 1312.9). Importantly, there was no effect of Context on pre-TMS muscle
260 activity ($F_{3,144}$ = 0.58, P = 0.629), which was below 10 μV in all contexts (baseline 5.5 ± 2.5 μV; irrelevant
261 5.8 ± 4.0 μV; nonselected 5.5 ± 2.7 μV; selected 5.8 ± 2.5 μV). Thus, participants' muscles rested during
262 action preparation, and differences in suprathreshold alpha motoneuron depolarization did not explain the
263 modulation of CS input-output (Devanne *et al.*, 1997).

264 *CS gain increases during response preparation for task-relevant representations*

265 The Slope of CS input-output differed significantly across Context ($F_{3,730}$ = 4.26, P = 0.00540).
266 Estimated Slope was greater in the selected context compared to baseline ($F_{1,730}$ = 5.42, P = 0.0404) and
267 the irrelevant context ($F_{1,730}$ = 9.76, P = 0.0111). Estimated Slope in the nonselected context was also
268 greater than the irrelevant context ($F_{1,730}$ = 5.87, P = 0.0404) but not baseline ($F_{1,730}$ = 2.79, P = 0.143).
269 There were no significant differences between baseline and irrelevant ($F_{1,730}$ = 0.95, P = 0.397) as well as
270 between nonselected and selected contexts ($F_{1,730}$ = 0.23, P = 0.628). Thus, context-dependent
271 multiplicative modulation of CS input-output was explained by an increase of Slope when the stimulated
272 motor representation was selected or nonselected for forthcoming action (i.e., task-relevant) compared to
273 baseline or when it was task-irrelevant (Figure 2b). Such nonlinear increases in sensitivity to excitatory
274 inputs are associated with response potentiation across sensory systems (Wood *et al.*, 2017).
275 Multiplicative gain modulation may be important for maximizing signal-to-noise and, computationally, can
276 extend the dynamic range of neuronal operations (Mitchell & Silver, 2003; Shine *et al.*, 2018). Of note is
277 that increased Slope was observed in both the selected and nonselected preparation contexts, indicating
278 a general role of gain modulation in potentiating task-relevant motor representations rather than

promoting effector-specific action selection. Overall, gain modulation may be pertinent for establishing the pool of candidate actions.

The Max of CS input-output also differed significantly across Context ($F_{3,730}$ = 24.04, P < 0.001). Estimated Max was greater in the selected context compared to irrelevant ($F_{1,730}$ = 14.62, P < 0.001) and nonselected ($F_{1,730}$ = 6.44, P = 0.0341) contexts, which did not differ from each other ($F_{1,730}$ = 1.89, P = 0.204). There were no differences between baseline and irrelevant ($F_{1,730}$ = 3.85, P = 0.0978), nonselected ($F_{1,730}$ = 0.40, P = 0.528), or selected ($F_{1,730}$ = 3.41, P = 0.0978) contexts. Thus, CS output maximum was greater during selected than nonselected and irrelevant contexts, but not baseline (Figure 2c). This pattern differed from that observed for the Slope and indicates the dynamic range of excitability in the CS pathway is influenced by more than gain adjustments alone.

Additive suppression of CS input-output in nonselected and task-irrelevant preparatory contexts

The Midpoint of CS input-output differed significantly across Context ($F_{3,730}$ = 11.48, P < 0.001). Estimated Midpoint was greater in the irrelevant context than baseline ($F_{1,730}$ = 7.00, P = 0.0125) and the selected context ($F_{1,730}$ = 18.54, P < 0.001). Estimated Midpoint in the nonselected context was also greater than baseline ($F_{1,730}$ = 9.65, P = 0.00393) and the selected context ($F_{1,730}$ = 25.32, P < 0.001). There was no significant difference between nonselected and irrelevant ($F_{1,730}$ = 0.05, P = 0.828) and between baseline and selected contexts ($F_{1,730}$ = 2.50, P = 0.137). Thus, context-dependent modulation of CS input-output was explained by an additive rightward shift of the Midpoint when the stimulated motor representation was task-irrelevant or nonselected for the forthcoming action compared to when it was selected (Figure 2d). The additive increase of the Midpoint during nonselected and irrelevant contexts was also greater than baseline, consistent with inhibition of CS input-output relative to intertrial rest (Derosiere & Duque, 2020). This nonspecific and apparently uniform suppression of irrelevant and nonselected motor representations may reflect widespread noise reduction within the CS pathway (Greenhouse *et al.*, 2015). These findings extend previous studies of preparatory inhibition and are consistent with a mechanism for enhancing the contrast of selected motor representations through the suppression of background activity.

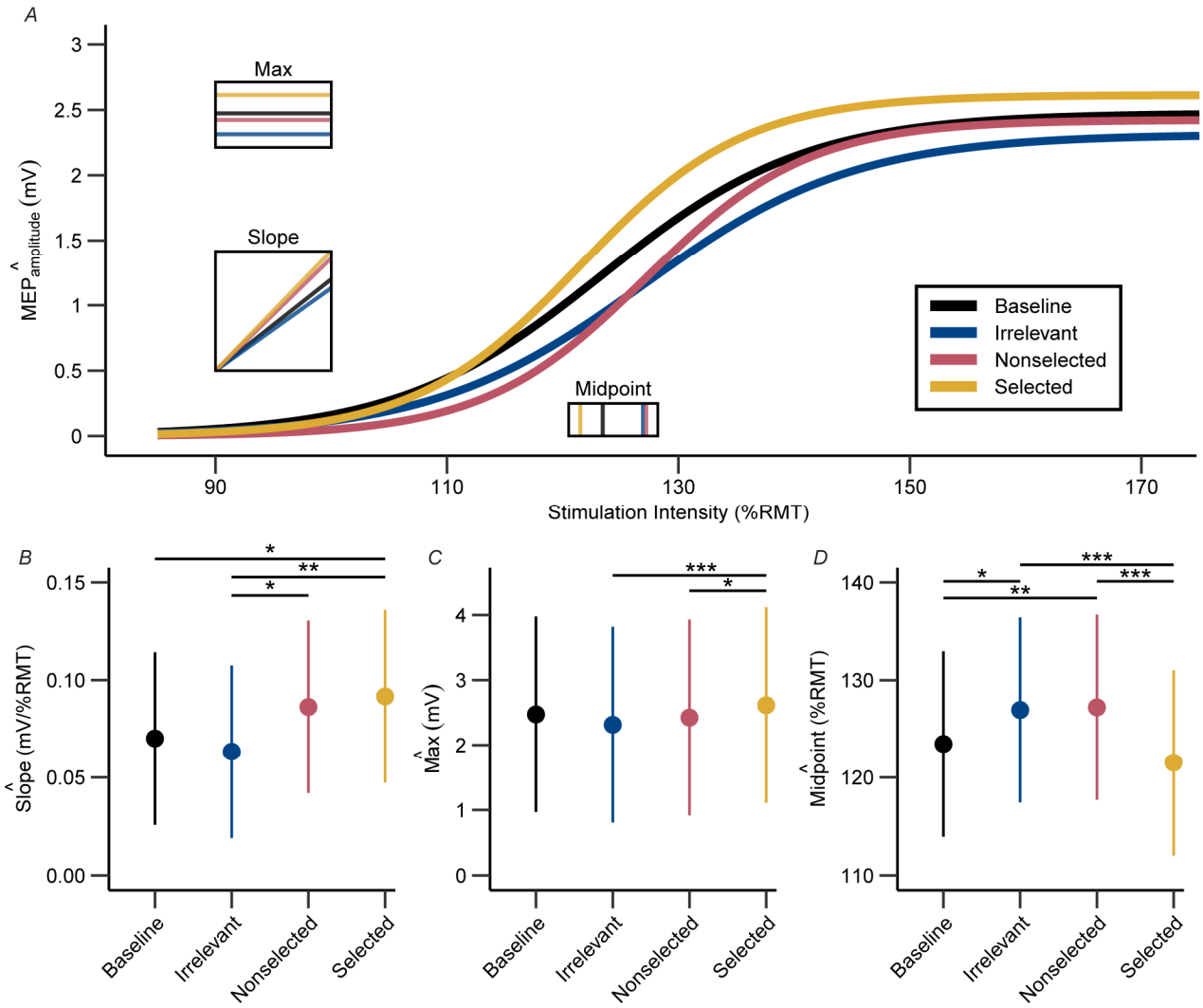

Figure 2: Modulation of CS input-output across goal-directed action preparation contexts. **a**, CS input-output curves across action preparation contexts. Insets indicate the model-derived Max, Slope, and Midpoint parameters used to generate the curves. **b**, Estimated Slope was greater in the selected context compared to baseline and irrelevant, greater in the nonselected context than irrelevant, with no significant differences between baseline and irrelevant or between nonselected and selected contexts. **c**, Estimated Max was greater in the selected context compared to the irrelevant and nonselected contexts, which did not differ from each other, with no differences between baseline and any other contexts. **d**, Estimated Midpoint was greater in the irrelevant and nonselected contexts compared to baseline and the selected context, with no significant differences between nonselected and irrelevant or between baseline and selected contexts. Data ranges represent mean ± standard deviation of the model-derived parameters in panels b – d, where the standard error reflects the precision of the estimated coefficients. Asterisks indicate statistical significance, where *P* is * < 0.05, ** < 0.01, *** < 0.001; n = 39 in all panels.

Preparatory suppression during goal-directed action preparation

Preparatory suppression, expressed as a reduced MEP amplitude relative to baseline, was observed during the irrelevant context across all stimulation intensities (110: $W = 615$, $P = 0.00374$; 130: $W = 573$, $P = 0.0293$; 150: $W = 608$, $P = 0.00546$; 170: $W = 616$, $P = 0.00354$), only at the 110 %RMT stimulation intensity during the nonselected context (110: $W = 644$, $P < 0.001$; 130: $W = 501$, $P = 0.372$; 150: $W = 411$, $P = 1.00$; 170: $W = 446$, $P = 1.00$), but at no stimulation intensity during the selected context (110: $W = 393$, $P = 1.00$; 130: $W = 238$, $P = 0.100$; 150: $W = 271$, $P = 0.296$; 170: $W = 280$, $P = 0.382$). Thus, preparatory suppression was observed across the entire input spectrum in the irrelevant context, only at the lower end of the input spectrum in the nonselected context and at no part of the input spectrum in the selected context (Figure 3a).

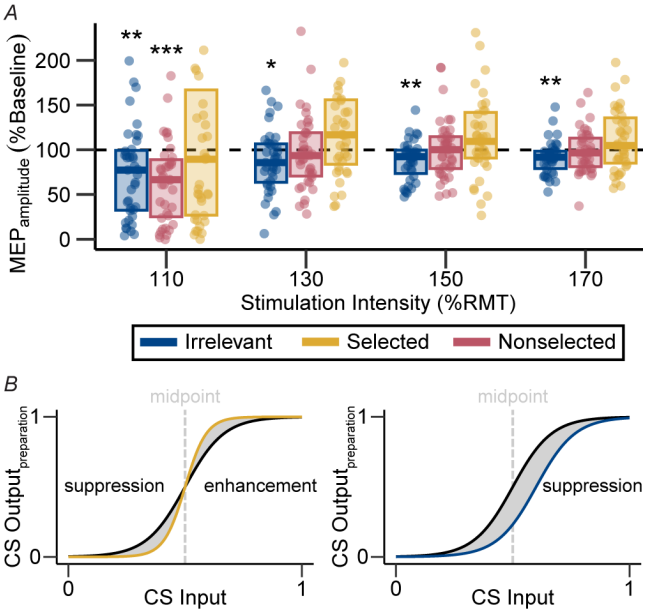

Figure 3: Preparatory suppression during goal-directed action preparation. **a**, Preparatory suppression, expressed as a reduced MEP amplitude relative to baseline, was observed during the irrelevant context across all stimulation intensities, only at the 110 %RMT stimulation intensity during the nonselected context, and at no stimulation intensity during the selected context. Crossbar boxes indicate sample median, 25th, and 75th percentiles. The dashed horizontal line indicates baseline MEP amplitude. Asterisks indicate statistical significance, where P is * < 0.05, ** < 0.01, *** < 0.001; n = 39. **b**, Conceptual overview of how CS input-output modulation can reflect preparatory suppression or enhancement depending on CS input and modulation. Here, assuming fixed alternative parameters, a multiplicative increase would be captured as preparatory suppression or enhancement at input intensities below or above the midpoint, respectively. In contrast, an additive increase (i.e., rightward shift) would be captured as preparatory suppression irrespective of the input intensity relative to the midpoint.

Gain modulation of CS input-output across preparatory contexts is associated with reaction time

Participants responded accurately and quickly during the behavioral tasks. There were no significant differences in accuracy across the response options during either go (nonstimulated: $X^2_3 = 4.82$, $P = 0.186$; stimulated: $X^2_3 = 5.10$, $P = 0.164$) or catch (nonstimulated: $X_2^3 = 3.00$, $P = 0.392$; stimulated: $X^2_3 = 3.12$, $P = 0.373$) trials, with a high average trial success indicating that participants performed the tasks correctly (Figure 4a). For EMG RT during nonstimulated trials, there was a significant

fixed effect of Task ($F_{1,114}$ = 10.18, P = 0.00183), with faster responses in the within-hand compared to the between-hand task. There was no fixed effect of Side ($F_{1,114}$ = 0.17, P = 0.684) or a Task × Side interaction ($F_{1,114}$ = 2.88, P = 0.0924). These EMG RT results were consistent during stimulated trials, whereby responses were faster in the within-hand compared to between-hand task ($F_{1,114}$ = 6.56, P = 0.0117), with no fixed effect of Side ($F_{1,114}$ = 0.15, P = 0.699) or a Task × Side interaction ($F_{1,114}$ = 0.63, P = 0.430). Thus, responses were faster when the prepared action involved a within-hand choice between the fingers of the dominant hand compared to a between-hand choice. However, RTs remained fast across all response alternatives (Figure 4b). Importantly, RTs were correlated between the two tasks for nonstimulated (r = 0.68, P < 0.001) and stimulated (r = 0.38, P < 0.001) trials, indicating individuals differed reliably in their RTs. There was a significant negative Pearson correlation between the Gain Index and EMG RT from nonstimulated (r = -0.32, P = 0.0449) and stimulated (r = -0.39, P = 0.0131) trials, whereby participants with a larger gain modulation index had faster RTs (Figure 4c). That is, participants who exhibited greater gain adjustments in the form of slope differences between task-relevant and task-irrelevant behavioral contexts were faster to initiate responses.

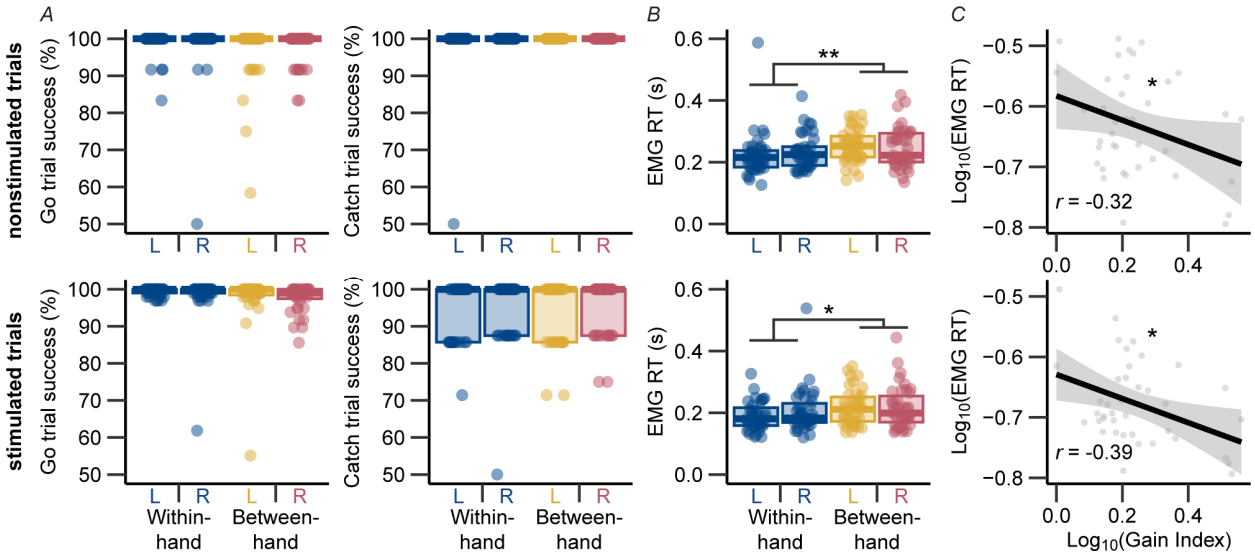

Figure 4: Behavioral performance during nonstimulated (*top*) and stimulated (*bottom*) trials and its relationship to CS input-output gain modulation. **a**, Accuracy during go (left) and catch (right) trials for which there was no significant effect of Response type on either measure. **b**, Response initiation times based on EMG were faster during the within-hand compared to the between-hand task. **c**, There was a significant negative Pearson correlation between Gain Index and EMG RT, whereby participants with greater gain in task-relevant than task-irrelevant action preparation contexts were faster responders. Crossbar boxes indicate sample median, 25th, and 75th percentiles. Asterisks indicate statistical significance, where P is * < 0.05, ** < 0.01; n = 39 in all panels.

CS input-output is not affected by participant sex or task order

CS input-output curves derived from the Sex model did not provide a better fit of the data than the null model (Sex AIC: 1319.1, Null AIC: 1312.9). There were no significant effects of Sex on estimated Max ($F_{1,736}$ = 0.61, P = 0.434), Slope ($F_{1,736}$ = 0.27, P = 0.605), or Midpoint ($F_{1,736}$ = 2.85, P = 0.0916) CS input-output parameters. CS input-output curves derived from the Order model also did not fit the data better than the null model (Order AIC: 1320.1). There were no significant effects of Order on estimated Max ($F_{1,736}$ = 0.04, P = 0.844), Slope ($F_{1,736}$ < 0.01, P = 0.944), or Midpoint ($F_{1,736}$ = 0.02, P = 0.876) CS input-output parameters. Thus, neither participant Sex nor task order influenced CS input-output during goal-directed action preparation (Figure 5).

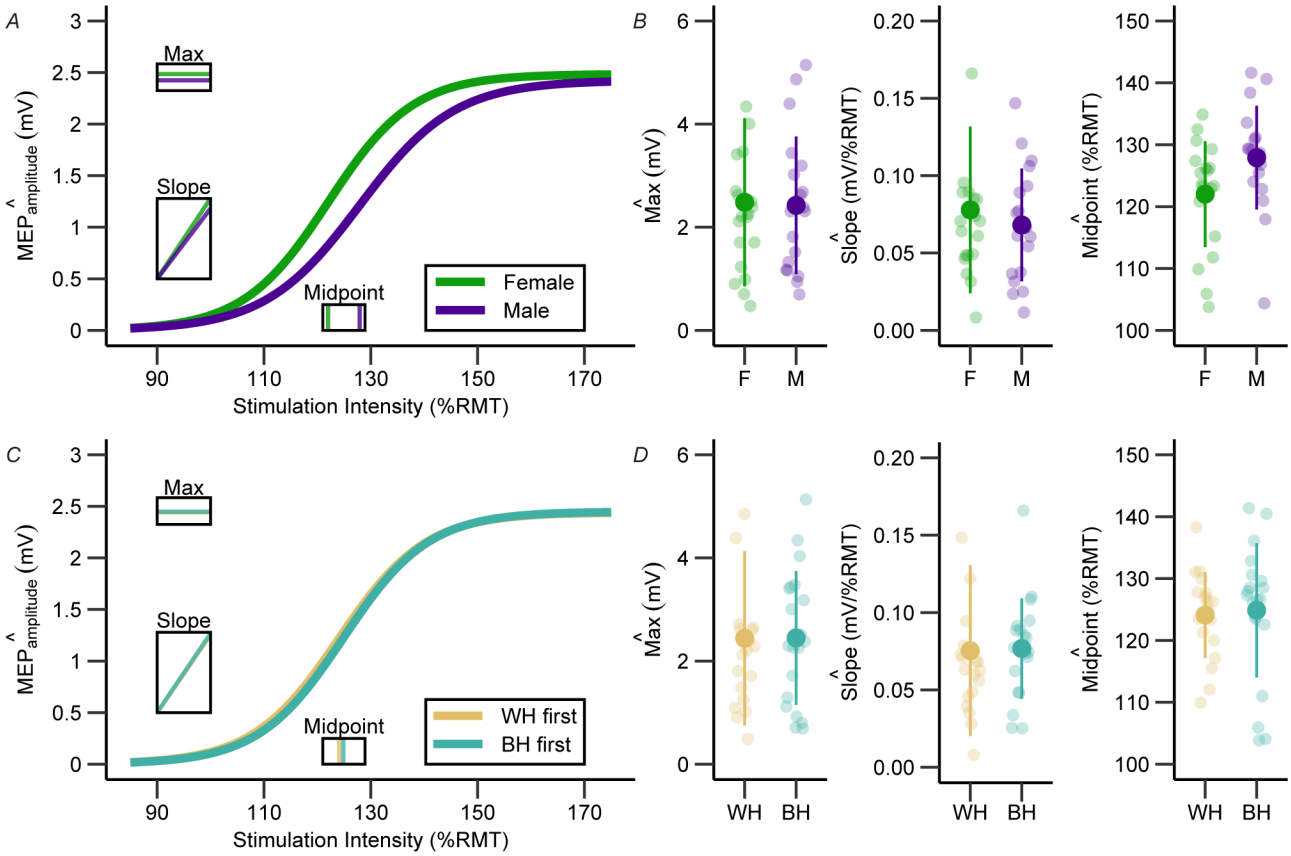

Figure 5: Modulation of CS input-output across participant sex and task order. **a**, CS input-out curves derived from the Sex model. **b**, There were no significant effects of Sex on estimated Max, Slope, or Midpoint CS input-output parameters. **c**, CS input-output curves derived from the Order model. **d**, Task order (WH: within-hand first; BH: between-hand first) had no significant effects on estimated Max, Slope, or Midpoint CS input-output parameters. Insets in subpanels a and c indicate estimated population means for the Max, Slope, and Midpoint parameters. Data ranges in subpanels b and d represent mean ± standard deviation of the model-derived parameters, where the standard error reflects the precision of the estimated coefficients. Individual datapoints indicate extracted participant-wise estimates of Max, Slope, and Midpoint parameters for between-subjects effects. n = 39 in all panels.

Discussion

The present study provides novel physiological evidence of multiplicative and additive neural computations within the human CS pathway during goal-directed action preparation. Specifically, we showed that the gain of behaviorally relevant motor representations (selected and non-selected) increases against a background of additive suppression of nonselected and task-irrelevant motor representations during goal-directed action preparation. Furthermore, the magnitude of gain modulation was associated with behavioral output, such that stronger modulators were faster responders. Below, we discuss the implications of these findings for understanding state-dependent computations within the human CS pathway during motor control.

Computational parallels between sensory and motor systems during action preparation

First, the findings indicate canonical computations well-described in sensory cortices (Salinas & Sejnowski, 2001; Mitchell & Silver, 2003; Silver, 2010) generalize to the human motor system. Previous work has established feature-based attention modulates gain within visual cortices (Treue & Trujillo, 1999), and normalization in the human visual system further supports attentional processes by theoretically separating figures from the ground (Bloem & Ling, 2019). Similar gain adjustments have been observed in the auditory cortex to increase spectrotemporal contrast (Rabinowitz *et al.*, 2011). Computational models of auditory (Mischler *et al.*, 2023) and visual (Polack *et al.*, 2013) sensory systems further indicate specific roles of gain for normalization and may mirror the contrast enhancement mechanism we propose operates within the CS pathway during action preparation. Such state-dependent gain adjustments for contrast enhancement could facilitate the transmission of descending signals along the CS pathway, similar to models of basal ganglia output for action selection (Nambu *et al.*, 2002). Importantly, while sensory and motor systems differ in their representational content and anatomy, they share critical functional similarities for guiding behavior (Hatsopoulos & Suminski, 2011). Therefore, contrast enhancement via simultaneously increased gain of behaviorally relevant and suppression of background neural representations may be a canonical motif for sculpting cortical circuit output.

The current findings also align with recurrent neural network models of the non-human primate motor cortex that indicate a specific role of gain modulation in moderating movement features such as speed (Stroud *et al.*, 2018). Such models are typically based on electrophysiological recordings from a neuronal subpopulation in a target region acquired without experimental control over the input strength to the efferent motor pathway. Here, by controlling the input intensity and tailoring it to each participant, we provide corroborative physiological evidence for these models by demonstrating that gain modulation along the human CS pathway during a preparatory state facilitates the execution of subsequent actions. Based on our data, we propose that increased gain of task-relevant motor representations occurs against a backdrop of suppressed nonselected and irrelevant motor representations to enhance the contrast between selected and bystander motor representations (Greenhouse *et al.*, 2015). We theorize this extension to existing models further promotes the initiation of prepared responses by increasing signal-to-noise within the CS pathway via divisive normalization (Figure 6). Our data can also inform computational models of the motor cortex by providing useful information about the dynamic range of physiological outputs and behavioral relationships in a human model. Translation of the context-dependent approach to other model systems can help evaluate whether CS input-output adjustments during an output-null (preparatory) motor state hasten the transition to an output-potent (execution) motor state (Hannah *et al.*, 2018; Churchland & Shenoy, 2024).

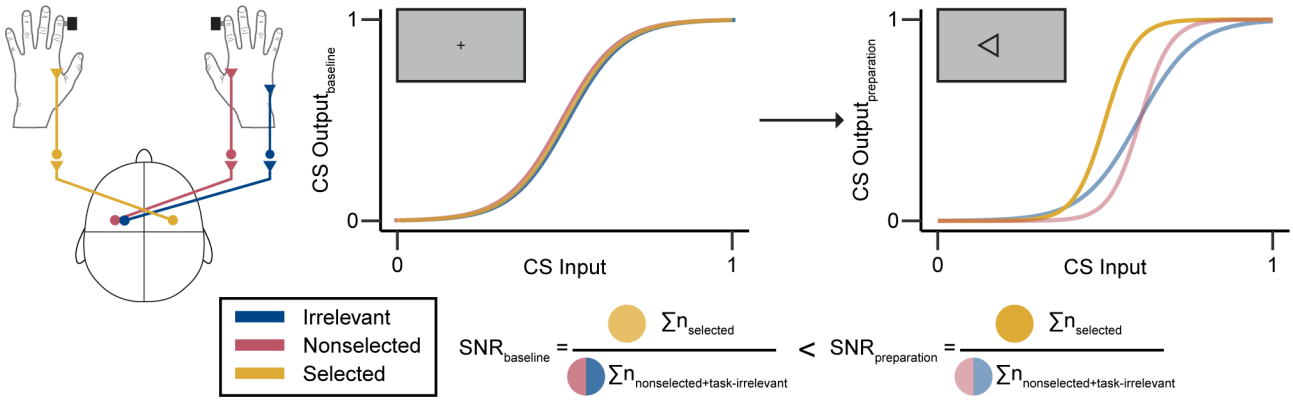

Figure 6: Theorized role of divisive normalization during goal-directed action preparation. CS input-output during action preparation depends upon task contexts. Schematized CS input-output plots represent the multiplicative increase in the selected and nonselected contexts and the additive increase in nonselected and task-irrelevant contexts. Speculatively, complementary multiplicative and additive changes can enhance the signal-to-noise ratio (SNR) between selected and bystander motor representations through divisive normalization to improve the fidelity of descending CS commands during action preparation.

Context-dependent computations with common coding frameworks

Context-dependent computations during goal-directed action preparation may fit within cognitive 'common coding' frameworks. These frameworks posit that human action control tasks are supported by internal representations ('event files') of stimulus-response relationships and their sensory effects (Hommel, 2009). Accordingly, action preparation entails retrieving an event file that triggers integrated neuronal processing across nonmotor and motor brain regions to prime action execution (Beste *et al.*, 2023). We observed neurophysiological evidence of corticospinal input-output computations recapitulated from sensory systems during action preparation, which may suggest a perception-action common code between motor and nonmotor systems. The current results, conceptualized within a common code framework, indicate that event files may have widespread motoric effects on not only the CS pathway to effectors involved directly in stimulus-response bindings but also suppression of task-irrelevant CS effector representations. In a somewhat homologous manner, modulation of sensory feedback during action control occurs at both spinal and supraspinal levels and can include a mixture of gain and suppression computations (Azim & Seki, 2019). Binding the motor command to anticipated perceptual feedback may occur via common gain modulation and suppression processes, with up-or-down regulation of neural pathways contingent upon their behavioral relevance (Frings *et al.*, 2020). Event file bindings are likely strong in the instructed-delay response task we employed; however, it is important to note that we did not set out to test event files explicitly and did not manipulate binding versus retrieval processes. Nevertheless, our findings raise the interesting possibility that gain increases in CS output during goal-directed action preparation are reciprocal to gain decreases in cutaneous feedback (Seki & Fetz, 2012) but coupled to gain increases in proprioceptive feedback during action execution (Confais *et al.*, 2017). Future work can investigate whether such changes arise from a common descending command.

Reevaluating context-dependent preparatory suppression across the CS input spectrum

An interesting observation from the current study was the lack of MEP suppression in the selected context. Previous TMS studies have observed *preparatory suppression* (i.e., reduced MEP amplitude below baseline during action preparation) across selected, nonselected, and task-irrelevant

466 contexts, albeit variably (Bundt & Huster, 2024). Our finding of enhanced CS gain in task-relevant
467 contexts may appear in conflict with inhibitory accounts (Ibáñez *et al.*, 2020). However, previous studies
468 often used a TMS intensity of ≤ 120 %RMT and, thus, only captured CS output at the lower end of the
469 input spectrum. By using a range of TMS intensities, we could model the entire CS input-output function,
470 providing a more complete picture of the underlying processes. Mathematically, both additive and
471 multiplicative changes in a sigmoidal input-output function would have complex effects on whether
472 context-dependent modulation is captured as suppression or enhancement when input intensity is below
473 or above the Midpoint (Figure 3b). We speculate that previous evidence of preparatory suppression of
474 task-relevant motor representations may result from TMS intensities below the CS input-output Midpoint.
475 Importantly, TMS may not mimic endogenous input to the CS pathway when transitioning from action
476 preparation to execution, which remains open for further investigation.

477 *Neural basis of context-dependent gain adjustments along the CS pathway*

478 Simultaneous gain adjustments and the suppression of background activity along the entire CS
479 pathway may rely on cooperative cortical, subcortical, and spinal mechanisms. For example, subcortical-
480 cortical projections from the thalamus to the prefrontal cortex selectively influence signal (figure) and
481 noise (ground) to guide cued behavior in the context of uncertainty via two distinct intracortical
482 mechanisms (Mukherjee *et al.*, 2021). Similar motifs may exist in thalamic projections to M1 to modulate
483 CS output (Halassa & Sherman, 2019). According to this framework, both increased gain of selected
484 motor representations and suppressed background activity would arise from a modulatory influence of
485 intracortical inhibitory circuits (Ferguson & Cardin, 2020). Alternatively, inhibition of background activity
486 may reflect the engagement of CS projections to spinal inhibitory neurons to suppress muscles that, if
487 activated, would interfere with the execution of the prepared action (Griffin & Strick, 2020).

488 Computations may also be mediated directly by spinal motoneurons, as MEPs measured with
489 surface EMG exhibit sigmoidal input-output properties, but individual spinal motor unit discharge rates
490 exhibit linear input-output properties (Devanne *et al.*, 1997). Summations across pools of spinal
491 motoneurons operating around the subliminal fringe may contribute to nonlinear transformations at the

population level (Di Lazzaro *et al.*, 1999), producing the sigmoidal shape modeled in our data. This account indicates that population-level activity of spinal motoneurons operating more closely to an activation threshold during action preparation could be responsible for the context-dependent gain changes we observed, independent of cortical mechanisms. However, evidence of altered corticospinal input-output properties, such as elevated gain in Parkinson's disease (Bologna *et al.*, 2018) and reduced maximum MEP output after stroke (Buetefisch *et al.*, 2018), underscores the importance of cortico-subcortical mechanisms. Therefore, it is likely that the observed CS input-output computations depend on cooperative cortical and spinal mechanisms rather than a single stage in the pathway.

Intra-hemispheric and inter-hemispheric mechanisms are engaged during action preparation (Derosiere & Duque, 2020) and undoubtedly contribute to the observed context-dependent computations. Regarding intra-hemispheric mechanisms, context-dependent computations may reflect distinct contributions to MEPs at varying TMS intensities. TMS-induced MEPs result from summated volleys of indirect (polysynaptic) and direct activation of pyramidal tract neurons along the CS pathway (Di Lazzaro *et al.*, 2012). The recruitment pattern is partially intensity-dependent, such that near-threshold TMS tends to evoke early indirect activation while increasing the intensity evokes later indirect activation and, ultimately, direct activation at high intensities (Di Lazzaro *et al.*, 2018). Thus, context-dependent CS input-output modulation may reflect changes in the relationship of indirect to direct waves due to the anatomical sources of MEPs (output) shifting with intensity (input). However, such changes could only be attributed to intrinsic differences between contexts, given the matched TMS intensities across the tasks. Inter-hemispheric projections via the corpus callosum are also engaged during action preparation (Hinder *et al.*, 2018; Wadsley *et al.*, 2023). Callosal projections in the mammalian brain are anatomically organized such that reciprocal projections to inhibitory interneurons and pyramidal tract neurons could support an interplay between excitatory and inhibitory processes (O'Hashi *et al.*, 2018). As such, contrast enhancement via simultaneous gain adjustments and 'crossed' surround inhibition may be an emergent functional property of inter-hemispheric connectivity in the motor system (for a detailed review, see Carson, 2020). The current study supports this integrative role of inter-hemispheric mechanisms given that nonselected and task-irrelevant computations both exhibited additive suppression but differed in gain, despite both being assessed in the opposite hemisphere of the selected effector. Ultimately, action

preparation likely requires integrated processing across intra-hemispheric and inter-hemispheric mechanisms to provide for truly context-dependent computations.

Limitations & Future Directions

The present study has some limitations. Using motor-evoked potentials (MEPs) elicited by TMS provides an accurate assay of CS output. However, when probed with single-pulse TMS, MEP modulation can arise from various mechanisms along the entire CS pathway, including intracortical, transcortical, subcortical, and spinal mechanisms (Duque *et al.*, 2017), which may have unique roles in action preparation (Derosiere & Duque, 2020). Thus, while we demonstrate that various computations manifest in CS output, we cannot disentangle the level of the motor system in which they arise. Future experiments will be able to determine at which level within the CS pathway these computations occur by leveraging multimodal approaches, such as paired-pulse TMS, to characterize better the multifaceted neuronal response to noninvasive brain stimulation and by studying clinical populations known to have CS input-output irregularities. Similarly, future experiments can record MEPs from task-irrelevant muscles within the same hemisphere as the selected effector to better determine the spatial specificity of CS input-output computations. This approach could also help disentangle the role of intra-hemispheric and inter-hemispheric mechanisms during action preparation.

Another limitation relates to in-task TMS only being delivered at baseline or a fixed time point late during action preparation. Limiting the temporal sampling was an important methodological choice to collect a reliable number of trials for accurate CS input-output modeling across various contexts. However, the time course of the observed computations during the transition from action preparation to execution remains unclear. Future experiments may employ methods to sample CS input-output effectively to enable a greater temporal resolution during action preparation (e.g., Alavi et al., 2019). Similarly, MEPs were recorded from only one muscle involved in the various response options, which limited comparisons of CS input-output computations with behavior. Future experiments may use advanced TMS techniques to simultaneously evaluate CS input-output in left and right M1 during action preparation (e.g., Vassiliadis et al., 2018).

The current work did not directly test relationships between the common coding framework and motor system anatomy. However, the observed mixture of context-dependent gain modulation and additive suppression may bridge these seemingly distinct concepts. Specifically, subcortical, intracortical, transcortical, or inter-hemispheric modulatory influences on the CS pathway might provide the neural infrastructure for common coding between sensory and motor areas (e.g., Takacs et al., 2021). Disruptions to these mechanisms could impair the perception-action common code for stimulus-response bindings. While this study does not favor one explanation over another, future studies mapping computations to neuroanatomical mechanisms could clarify how event files are instantiated and retrieved during action preparation.

Conclusion

The present study aimed to test the presence of multiplicative and additive computations in human CS input-output during goal-directed action preparation. We provided physiological evidence that goal-directed action preparation of finger responses entails a mixture of input-output computations within the human motor system. These computations are context-dependent, characterized by gain increases in task-relevant motor representations against a backdrop of suppression in bystander motor representations, potentially facilitating action initiation through contrast enhancement. The recapitulation of canonical neural computations across motor and non-motor neuronal circuits suggests that these processes may generalize throughout the human nervous system.

Additional information

Data availability statement: The data and reproducible code that support the findings of this study are openly available in OSF at https://osf.io/837ms

Acknowledgments: The authors thank Kate Bakken, Mitch Fisher, Charlie Lewkowitz, Hayami Nishio, Michelle Ortman, and Tania Sarabia for their help with data collection and preprocessing. The authors also thank Luca Mazzucato and Richard Ivry for their helpful feedback on this manuscript.

Author contributions: Conceptualization, C.G.W and I.G.; Methodology, C.G.W, T.N., and I.G.; Formal Analysis, C.G.W. and T.N.; Investigation, C.G.W. and C.H.; Writing – Original Draft, C.G.W. and I.G.;

Writing – Reviewing & Editing, C.G.W, T.N., C.H., and I.G.; Visualization, C.G.W.; Supervision, I.G.; Funding acquisition, I.G.

Competing interests: The authors declare no competing interests.

Funding: This research was supported by NIH grant NINDS R01NS123115.

References

Alavi SMM, Goetz SM & Peterchev A V. (2019). Optimal Estimation of Neural Recruitment Curves Using Fisher Information: Application to Transcranial Magnetic Stimulation. *IEEE Transactions on Neural Systems and Rehabilitation Engineering* **27,** 1320–1330.

Allman J, Miezin F & McGuinness E (1985). Stimulus Specific Responses from Beyond the Classical Receptive Field: Neurophysiological Mechanisms for Local-Global Comparisons in Visual Neurons. *Annu Rev Neurosci* **8,** 407–430.

Angelucci A, Bijanzadeh M, Nurminen L, Federer F, Merlin S & Bressloff PC (2017). Circuits and Mechanisms for Surround Modulation in Visual Cortex. *Annu Rev Neurosci* **40,** 425–451.

Aungst JL, Heyward PM, Puche AC, Karnup S V., Hayar A, Szabo G & Shipley MT (2003). Centre–surround inhibition among olfactory bulb glomeruli. *Nature* **426,** 623–629.

Azim E & Seki K (2019). Gain control in the sensorimotor system. *Curr Opin Physiol* **8,** 177–187.

Bakken K, Horton C, Fisher M, Wadsley CG & Greenhouse I (2024). Corticospinal excitability at rest outside of a task does not differ from task intertrial intervals in healthy adults. *Exp Brain Res* **242,** 2263–2270.

Beste C, Münchau A & Frings C (2023). Towards a systematization of brain oscillatory activity in actions. *Commun Biol* **6,** 137.

Bestmann S & Duque J (2016). Transcranial Magnetic Stimulation. *The Neuroscientist* **22,** 392–405.

Bloem IM & Ling S (2019). Normalization governs attentional modulation within human visual cortex. *Nat Commun* **10,** 5660.

596 Bologna M, Guerra A, Paparella G, Giordo L, Alunni Fegatelli D, Vestri AR, Rothwell JC & Berardelli A
597 (2018). Neurophysiological correlates of bradykinesia in Parkinson's disease. *Brain* **141,** 2432–
598 2444.

599 Buetefisch CM, Revill KP, Haut MW, Kowalski GM, Wischnewski M, Pifer M, Belagaje SR, Nahab F,
600 Cobia DJ, Hu X, Drake D & Hobbs G (2018). Abnormally reduced primary motor cortex output is
601 related to impaired hand function in chronic stroke. *J Neurophysiol* **120,** 1680–1694.

602 Bundt C & Huster RJ (2024). Corticospinal excitability reductions during action preparation and action
603 stopping in humans: Different sides of the same inhibitory coin? *Neuropsychologia* **195,** 108799.

604 Carandini M & Heeger DJ (2012). Normalization as a canonical neural computation. *Nat Rev Neurosci* **13,**
605 51–62.

606 Carson RG (2020). Inter-hemispheric inhibition sculpts the output of neural circuits by co-opting the two
607 cerebral hemispheres. *J Physiol* **598,** 4781–4802.

608 Churchland MM & Shenoy K V. (2024). Preparatory activity and the expansive null-space. *Nat Rev*
609 *Neurosci* **25,** 213–236.

610 Confais J, Kim G, Tomatsu S, Takei T & Seki K (2017). Nerve-Specific Input Modulation to Spinal
611 Neurons during a Motor Task in the Monkey. *The Journal of Neuroscience* **37,** 2612–2626.

612 Derosiere G & Duque J (2020). Tuning the Corticospinal System: How Distributed Brain Circuits Shape
613 Human Actions. *The Neuroscientist* **26,** 359–379.

614 Devanne H, Lavoie BA & Capaday C (1997). Input-output properties and gain changes in the human
615 corticospinal pathway. *Exp Brain Res* **114,** 329–338.

616 Duque J, Greenhouse I, Labruna L & Ivry RB (2017). Physiological Markers of Motor Inhibition during
617 Human Behavior. *Trends Neurosci* **40,** 219–236.

618 Duque J & Ivry RB (2009). Role of Corticospinal Suppression during Motor Preparation. *Cerebral Cortex*
619 **19,** 2013–2024.

620 Ferguson KA & Cardin JA (2020). Mechanisms underlying gain modulation in the cortex. *Nat Rev*
621 *Neurosci* **21,** 80–92.

622 Foeller E, Celikel T & Feldman DE (2005). Inhibitory Sharpening of Receptive Fields Contributes to
623 Whisker Map Plasticity in Rat Somatosensory Cortex. *J Neurophysiol* **94,** 4387–4400.

624 Foltys H, Sparing R, Boroojerdi B, Krings T, Meister IG, Mottaghy FM & Töpper R (2001). Motor control in
625 simple bimanual movements: a transcranial magnetic stimulation and reaction time study. *Clinical*
626 *Neurophysiology* **112,** 265–274.

627 Frings C, Hommel B, Koch I, Rothermund K, Dignath D, Giesen C, Kiesel A, Kunde W, Mayr S, Moeller B,
628 Möller M, Pfister R & Philipp A (2020). Binding and Retrieval in Action Control (BRAC). *Trends Cogn*
629 *Sci* **24,** 375–387.

630 Georgopoulos AP & Stefanis CN (2007). Local shaping of function in the motor cortex: Motor contrast,
631 directional tuning. *Brain Res Rev* **55,** 383–389.

632 Gilday OD, Praegel B, Maor I, Cohen T, Nelken I & Mizrahi A (2023). Surround suppression in mouse
633 auditory cortex underlies auditory edge detection. *PLoS Comput Biol* **19,** e1010861.

634 Greenhouse I (2022). Inhibition for gain modulation in the motor system. *Exp Brain Res* **240,** 1295–1302.

635 Greenhouse I, Sias A, Labruna L & Ivry RB (2015). Nonspecific Inhibition of the Motor System during
636 Response Preparation. *Journal of Neuroscience* **35,** 10675–10684.

637 Griffin DM & Strick PL (2020). The motor cortex uses active suppression to sculpt movement. *Sci Adv*;
638 DOI: 10.1126/sciadv.abb8395.

Halassa MM & Sherman SM (2019). Thalamocortical Circuit Motifs: A General Framework. *Neuron* **103,** 762–770.

Hannah R, Cavanagh SE, Tremblay S, Simeoni S & Rothwell JC (2018). Selective Suppression of Local Interneuron Circuits in Human Motor Cortex Contributes to Movement Preparation. *The Journal of Neuroscience* **38,** 1264–1276.

Hatsopoulos NG & Suminski AJ (2011). Sensing with the Motor Cortex. *Neuron* **72,** 477–487.

Heusser K, Heusser R, Jordan J, Urechie V, Diedrich A & Tank J (2021). Baroreflex Curve Fitting Using a WYSIWYG Boltzmann Sigmoidal Equation. *Front Neurosci*; DOI: 10.3389/fnins.2021.697582.

Hillyard SA, Vogel EK & Luck SJ (1998). Sensory gain control (amplification) as a mechanism of selective attention: electrophysiological and neuroimaging evidence. *Philos Trans R Soc Lond B Biol Sci* **353,** 1257–1270.

Hinder MR, Puri R, Kemp S, Waitzer S, Reissig P, Stöckel T & Fujiyama H (2018). Distinct modulation of interhemispheric inhibitory mechanisms during movement preparation reveals the influence of cognition on action control. *Cortex* **99,** 13–29.

Hommel B (2009). Action control according to TEC (theory of event coding). *Psychological Research Psychologische Forschung* **73,** 512–526.

Ibáñez J, Hannah R, Rocchi L & Rothwell JC (2020). Premovement Suppression of Corticospinal Excitability may be a Necessary Part of Movement Preparation. *Cerebral Cortex* **30,** 2910–2923.

Jackson N & Greenhouse I (2019). VETA: An Open-Source Matlab-Based Toolbox for the Collection and Analysis of Electromyography Combined With Transcranial Magnetic Stimulation. *Front Neurosci*; DOI: 10.3389/fnins.2019.00975.

Katzner S, Busse L & Carandini M (2011). $GABA_A$ Inhibition Controls Response Gain in Visual Cortex. *The Journal of Neuroscience* **31,** 5931–5941.

662 Kaufman MT, Churchland MM, Santhanam G, Yu BM, Afshar A, Ryu SI & Shenoy K V. (2010). Roles of
663 Monkey Premotor Neuron Classes in Movement Preparation and Execution. *J Neurophysiol* **104,**
664 799–810.

665 Kaufman MT, Churchland MM & Shenoy K V. (2013). The roles of monkey M1 neuron classes in
666 movement preparation and execution. *J Neurophysiol* **110,** 817–825.

667 Kukke SN, Paine RW, Chao C-C, de Campos AC & Hallett M (2014). Efficient and Reliable
668 Characterization of the Corticospinal System Using Transcranial Magnetic Stimulation. *Journal of*
669 *Clinical Neurophysiology* **31,** 246–252.

670 Di Lazzaro V, Oliviero A, Profice P, Insola A, Mazzone P, Tonali P & Rothwell JC (1999). Effects of
671 voluntary contraction on descending volleys evoked by transcranial electrical stimulation over the
672 motor cortex hand area in conscious humans. *Exp Brain Res* **124,** 525–528.

673 Di Lazzaro V, Profice P, Ranieri F, Capone F, Dileone M, Oliviero A & Pilato F (2012). I-wave origin and
674 modulation. *Brain Stimul* **5,** 512–525.

675 Di Lazzaro V, Rothwell J & Capogna M (2018). Noninvasive Stimulation of the Human Brain: Activation of
676 Multiple Cortical Circuits. *The Neuroscientist* **24,** 246–260.

677 Lebon F, Greenhouse I, Labruna L, Vanderschelden B, Papaxanthis C & Ivry RB (2016). Influence of
678 Delay Period Duration on Inhibitory Processes for Response Preparation. *Cerebral Cortex* **26,**
679 2461–2470.

680 Lee S-H, Kwan AC, Zhang S, Phoumthipphavong V, Flannery JG, Masmanidis SC, Taniguchi H, Huang
681 ZJ, Zhang F, Boyden ES, Deisseroth K & Dan Y (2012). Activation of specific interneurons improves
682 V1 feature selectivity and visual perception. *Nature* **488,** 379–383.

Merchant H, Naselaris T & Georgopoulos AP (2008). Dynamic Sculpting of Directional Tuning in the Primate Motor Cortex during Three-Dimensional Reaching. *The Journal of Neuroscience* **28,** 9164–9172.

Mischler G, Keshishian M, Bickel S, Mehta AD & Mesgarani N (2023). Deep neural networks effectively model neural adaptation to changing background noise and suggest nonlinear noise filtering methods in auditory cortex. *Neuroimage* **266,** 119819.

Mitchell SJ & Silver RA (2003). Shunting Inhibition Modulates Neuronal Gain during Synaptic Excitation. *Neuron* **38,** 433–445.

Mukherjee A, Lam NH, Wimmer RD & Halassa MM (2021). Thalamic circuits for independent control of prefrontal signal and noise. *Nature* **600,** 100–104.

Nambu A, Tokuno H & Takada M (2002). Functional significance of the cortico–subthalamo–pallidal 'hyperdirect' pathway. *Neurosci Res* **43,** 111–117.

O'Hashi K, Fekete T, Deneux T, Hildesheim R, van Leeuwen C & Grinvald A (2018). Interhemispheric Synchrony of Spontaneous Cortical States at the Cortical Column Level. *Cerebral Cortex* **28,** 1794–1807.

Pi H-J, Hangya B, Kvitsiani D, Sanders JI, Huang ZJ & Kepecs A (2013). Cortical interneurons that specialize in disinhibitory control. *Nature* **503,** 521–524.

Polack P-O, Friedman J & Golshani P (2013). Cellular mechanisms of brain state–dependent gain modulation in visual cortex. *Nat Neurosci* **16,** 1331–1339.

Pouget A & Snyder LH (2000). Computational approaches to sensorimotor transformations. *Nat Neurosci* **3,** 1192–1198.

Prut Y & Fetz EE (1999). Primate spinal interneurons show pre-movement instructed delay activity. *Nature* **401,** 590–594.

Rabinowitz NC, Willmore BDB, Schnupp JWH & King AJ (2011). Contrast Gain Control in Auditory Cortex. *Neuron* **70,** 1178–1191.

Salinas E & Sejnowski TJ (2001). Book Review: Gain Modulation in the Central Nervous System: Where Behavior, Neurophysiology, and Computation Meet. *The Neuroscientist* **7,** 430–440.

Salinas E & Thier P (2000). Gain Modulation. *Neuron* **27,** 15–21.

Seki K & Fetz EE (2012). Gating of Sensory Input at Spinal and Cortical Levels during Preparation and Execution of Voluntary Movement. *The Journal of Neuroscience* **32,** 890–902.

Shine JM, Aburn MJ, Breakspear M & Poldrack RA (2018). The modulation of neural gain facilitates a transition between functional segregation and integration in the brain. *Elife*; DOI: 10.7554/eLife.31130.

Silbert BI, Patterson HI, Pevcic DD, Windnagel KA & Thickbroom GW (2013). A comparison of relative-frequency and threshold-hunting methods to determine stimulus intensity in transcranial magnetic stimulation. *Clinical Neurophysiology* **124,** 708–712.

Silver RA (2010). Neuronal arithmetic. *Nat Rev Neurosci* **11,** 474–489.

Sohn YoungH & Hallett M (2004). Surround inhibition in human motor system. *Exp Brain Res*; DOI: 10.1007/s00221-004-1909-y.

Soteropoulos DS (2018). Corticospinal gating during action preparation and movement in the primate motor cortex. *J Neurophysiol* **119,** 1538–1555.

Stinear CM & Byblow WD (2003). Role of Intracortical Inhibition in Selective Hand Muscle Activation. *J Neurophysiol* **89,** 2014–2020.

Stroud JP, Porter MA, Hennequin G & Vogels TP (2018). Motor primitives in space and time via targeted gain modulation in cortical networks. *Nat Neurosci* **21,** 1774–1783.

728 Takacs A, Bluschke A, Kleimaker M, Münchau A & Beste C (2021). Neurophysiological mechanisms
729 underlying motor feature binding processes and representations. *Hum Brain Mapp* **42,** 1313–1327.

730 Treue S & Trujillo JCM (1999). Feature-based attention influences motion processing gain in macaque
731 visual cortex. *Nature* **399,** 575–579.

732 Vassiliadis P, Grandjean J, Derosiere G, de Wilde Y, Quemener L & Duque J (2018). Using a Double-Coil
733 TMS Protocol to Assess Preparatory Inhibition Bilaterally. *Front Neurosci*; DOI:
734 10.3389/fnins.2018.00139.

735 Wadsley CG, Cirillo J, Nieuwenhuys A & Byblow WD (2023). Proactive Interhemispheric Disinhibition
736 Supports Response Preparation during Selective Stopping. *The Journal of Neuroscience* **43,** 1008–
737 1017.

738 Wang X, Liu Y, Li X, Zhang Z, Yang H, Zhang Y, Williams PR, Alwahab NSA, Kapur K, Yu B, Zhang Y,
739 Chen M, Ding H, Gerfen CR, Wang KH & He Z (2017). Deconstruction of Corticospinal Circuits for
740 Goal-Directed Motor Skills. *Cell* **171,** 440-455.e14.

741 Wang Y, Shanbhag SJ, Fischer BJ & Pena JL (2012). Population-Wide Bias of Surround Suppression in
742 Auditory Spatial Receptive Fields of the Owl's Midbrain. *Journal of Neuroscience* **32,** 10470–10478.

743 Welniarz Q, Dusart I & Roze E (2017). The corticospinal tract: Evolution, development, and human
744 disorders. *Dev Neurobiol* **77,** 810–829.

745 Wood KC, Blackwell JM & Geffen MN (2017). Cortical inhibitory interneurons control sensory processing.
746 *Curr Opin Neurobiol* **46,** 200–207.

747 Xu J, Mawase F & Schieber MH (2024). Evolution, biomechanics, and neurobiology converge to explain
748 selective finger motor control. *Physiol Rev* **104,** 983–1020.

749 Zagha E, Ge X & McCormick DA (2015). Competing Neural Ensembles in Motor Cortex Gate Goal-
750 Directed Motor Output. *Neuron* **88,** 565–577.

751